

A NON-HOMOGENEOUS POISSON PROCESS MODEL OF SKIN CONDUCTANCE RESPONSES INTEGRATED WITH OBSERVED REGULATORY BEHAVIORS FOR AUTISM INTERVENTION

Theodora Chaspari¹, Matthew Goodwin², Oliver Wilder-Smith², Amanda Gulrud³,
Charlotte A. Mucchetti³, Connie Kasari³, Shrikanth Narayanan¹

¹ University of Southern California, Los Angeles, CA, USA

² Northeastern University, Boston, MA, USA

³ University of California, Los Angeles, CA, USA

chaspari@usc.edu, m.goodwin@neu.edu, wilder-smith.o@husky.neu.edu, agulrud@mednet.ucla.edu,
cmucchetti@mednet.ucla.edu, kasari@gseis.ucla.edu, shri@sipi.usc.edu

ABSTRACT

Early intervention in individuals with Autism Spectrum Disorder (ASD) can improve core and associated symptoms and facilitate skills that increase social opportunities. However, determining effective intervention success in this population, and the mechanisms that produce it, is currently restricted to observable behavior. The need of therapy assessment metrics beyond traditional behavioral criteria, led to the use of physiological signals for capturing child-therapist internal dynamics during an intervention session. Internal physiological states were measured through Electrodermal Activity (EDA) and modeled in relation to observed self- and co-regulatory behaviors. A common measure of EDA, Skin Conductance Response (SCR), was the primary signal of interest and assumed to form a non-homogeneous Poisson Process whose rate function is determined by observed regulatory behaviors. Through likelihood and residual goodness of fit analysis, statistical tests and classification tasks, our results indicate that SCR changes and observable behavior in child-therapist dyads are temporally associated and the estimated model parameters can be linked to the types of regulation stimuli.

Index Terms— Electrodermal Activity, Skin Conductance Response, Non-homogeneous Poisson Process, Residual Analysis, Autism Intervention, Regulation

1. INTRODUCTION

Autism Spectrum Disorder (ASD) constitutes a heterogeneous class of developmental disabilities characterized by persistent impairments in social-communication skills accompanied by restrictive and repetitive patterns of behaviors and interests. Individuals with ASD often benefit across the lifespan from intensive behavioral interventions targeting the core domains of the disorder. Recent advancements in these behavioral intervention approaches have led to several well-established treatments [1, 2], but the large heterogeneity in ASD phenotypes results in considerable variability in outcomes.

One important factor in ASD therapy is the fit between the child and the treatment and/or the therapist. This can potentially be examined by measuring child and therapist co-regulation during intervention sessions. Emotion co-regulation is defined as the “extrinsic and intrinsic processes responsible for monitoring, evaluating and modifying emotional reactions” [3, 4].

Despite the neurobiological roots of ASD [5], assessment of treatment is largely based upon behavioral coding of the child’s social-communication skills and restricted-repetitive behaviors [6]. An understudied domain is the physiological dynamics within and

between a child and a therapist during and across intervention to determine therapeutic mechanisms of change and behavioral outcomes.

Internal physiological indices can provide a complementary view of mechanisms that support behavioral interaction and affect displays in children with ASD [7]. Electrodermal Activity (EDA) is a physiological index of sympathetic nervous system arousal recorded through sweat secretion at the surface of the skin. Changes in EDA have been linked to affective, cognitive, and sensory processing in humans [8, 9]. Simultaneous monitoring of a child’s and therapist’s EDA and behavioral responses permits exploration of each person’s internal state, how those states interact with observable behavior and how interpersonal bio-behavioral dynamics evolve over the course of therapy. These can be modeled, quantified and potentially assessed from EDA signals using emerging signal processing techniques, that can afford us new insights into better understanding typical and atypical behavioral patterns [10].

In the current study, we model EDA signals as a time sequence of Skin Conductance Responses (SCRs) (i.e. high frequency fluctuations in EDA) affected by external observable coexisting events. SCR occurrences form a spike train modeled by a non-homogeneous Poisson Process (PP), whose rate function incorporates external factors, such as child emotion self-regulation and therapist emotional co-regulation instances. We evaluate our model using pilot data of intervention sessions from the UCLA Center for Autism and Research Treatment. We hypothesize that incorporating information from external regulatory behaviors will result in better modeling child and therapist EDA. Likelihood and residual analysis are performed to assess the goodness of fit of the proposed model to our data. Analysis of the PP rate function parameters with statistical tests and visual inspection implies that self- and co-regulation events affect the child and therapist physiological state differently. Classification results further indicate that the PP parameters can be informative about the types of behaviors occurring during the intervention.

2. RELATION TO PRIOR WORK

PPs have been the focus of many studies examining event incidents across a diverse set of applications. Ogata [11] proposed a non-homogeneous PP with rate function being the sum of modulated exponentials for earthquake occurrence. A piece-wise linear rate function was used to estimate the number of telephone calls in the AT&T network [12]. Point processes have also captured software failures [13] and heartbeat intervals [14]. To the best of our knowledge, this is the first study modeling neuro-physiological EDA sig-

Table 1. Distribution of child self-regulatory and therapist co-regulatory behaviors for each participant.

Self-Regulatory Behaviors		Participant		
Code	Description	1	2	3
1	Symbolic Self-Soothing	0	0	2
2	Physical Self-Soothing	1	0	0
3	Repetitive Behavior	0	0	0
4	Tension Release	0	0	4
5	Avoidance	0	1	0
6	Distraction	0	2	3
7	Therapist Orientation	0	17	7
8	Other-Directed Comfort Seeking	0	0	0
9	Other-Directed Assistance Seeking	0	2	2
Total		1	22	18

Co-Regulatory Behaviors		Participant		
Code	Description	1	2	3
1	Active Game-Like Engagement	0	0	0
2	Redirection of Attention	0	2	5
3	Reassurance	1	5	4
4	Following	0	7	12
5	Physical Comfort	0	1	5
Total		1	15	26

nals (herein, SCR occurrences) with PPs.

Quantifying human interaction with signal processing techniques has recently gained a lot of interest. Lee et al. [15] used acoustic features to model couple’s entrainment during marital therapy sessions. Acoustic and linguistic cues have also been analysed in terms of child and therapist interactions [16, 17, 18]. Finally, Young et al. [19] examined the coordination of body language behavior between actors during improvised interactions.

3. DATA DESCRIPTION AND ANNOTATION

Our paper includes data from three minimally-verbal male participants with ASD who were receiving treatment at the UCLA Center for Autism and Research Treatment. EDA was captured from the child’s and therapist’s wrist using the Affectiva Q-Sensor [20] with 32Hz sampling rate. Each child participated in one videotaped session of approximately 30min with the same therapist.

All sessions were coded by an expert for child emotion self-regulation and therapist co-regulation strategies based on [4], whose types and per participant distribution are shown in Table 1. The variability across the three children led to different annotation results. For Participant 1, the absence of any negativity resulted to only one self- and one co-regulation episode coded.

4. MODEL DESCRIPTION

4.1. EDA Background

EDA is widely used in clinical research as a marker of normal and abnormal behavior [21, 22]. It is decomposed into a slow moving component, which depicts a general trend and is called Skin Conductance Level (SCL), and a fast moving part or SCR, containing the fluctuations superimposed into the tonic signal (Fig. 1a). SCRs can occur in the absence of identifiable stimuli and after the presentation of a novel or unexpected event [23]. Here we model SCR time sequences, as an indicator of specific or non-specific stimuli and explain it with external observable behaviors. We do not take into account other common EDA metrics (SCR amplitude, rise/recovery time, etc.), although intend to do so in future work.

4.2. Rate Function Description

PPs have been widely used to model event occurrence. Since inter-arrival time between SCRs can be thought of as waiting time, we chose to model SCR incidents as a spike train (Fig. 1b) that form a PP (Fig. 1c), increasing by one every time a SCR spike occurs.

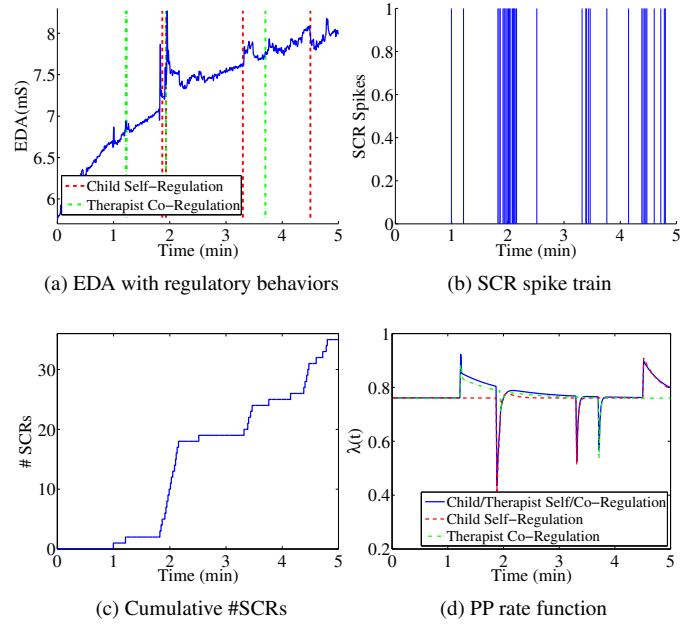


Fig. 1. Example of modeling Skin Conductance Response (SCR) occurrence of Electrodermal Activity (EDA) in relation to child/psychologist self/co-regulatory behaviors with a non-homogeneous Poisson Process (PP).

During child-therapist intervention sessions, we assume two PP parts. The first is a homogeneous PP with SCRs occurring as a result of non-specific events for which we do not have behavioral annotation. The second consists of a non-homogeneous PP, where SCR occurrences are linked to external annotated self- and co-regulatory behaviors of the child and therapist. Thus the PP rate function is:

$$\lambda(t) = \lambda_0 + \sum_{k=1}^K g_k(t - \tau_k) \quad (1)$$

In Eq. 1, λ_0 is the parameter of the homogeneous PP, K are the total annotated behaviors, τ_k are the time occurrences of self/co-regulation events and $g_k(t)$ are the functions introducing the non-homogeneity of the PP caused by the observable regulatory behaviors. These affect the SCR rate from time τ_k and onwards. Since it is reasonable to assume their short-term influence on EDA, g_k can be modeled as an exponential with amplitude λ_k and rate α_k (Fig. 1d):

$$g_k(t) = \lambda_k e^{-\alpha_k t} u(t) \quad (2)$$

where $u(t) = 1, t \geq 0$ and $u(t) = 0, t < 0$. In our terminology, the word “rate” is used to describe the PP rate function $\lambda(t)$ (Eq. 1) and also the change rate α_k (Eq. 2) of the exponential function. We refer to α_k as the “exponential change rate” and $\lambda(t)$ as the “PP rate function.” Eq. 2 assumes that each behavior k influences the SCR rate differently. The exponential function was chosen since it provides a smooth transition to the homogeneous PP with rate λ_0 .

4.3. Parameter Estimation

The parameters $\theta = [\lambda_0 \lambda_1 \dots \lambda_K \alpha_1 \dots \alpha_K]$ are estimated with Least Mean Squares (LMS) as in [12]. The PP is sampled by counting the number of SCR arrivals in subintervals $s_n = \left(\frac{(n-1)T}{N}, \frac{nT}{N} \right]$,

Table 2. Likelihood and residual goodness of fit measures for the Poisson Process model of child and therapist Skin Conductance Responses (SCRs) based on child self-regulatory (Self-Reg.) and therapist co-regulatory (Co-Reg.) behaviors.

Participant	Metric	Child SCR				Therapist SCR			
		Homogeneous	Child Self-Reg.	Therapist Co-Reg.	Child-Therapist Self/Co-Reg.	Homogeneous	Child Self-Reg.	Therapist Co-Reg.	Child-Therapist Self/Co-Reg.
1	# Parameters	1	3	3	5	1	3	3	5
	Log-Likelihood	-1892	-1891	-1892	-1891	-1882	-1882	-1882	-1882
	AIC	3785	3789	3789	3793	3766	3769	3770	3773
	KS Statistic 1 ($\times 10^{-3}$)	6.4	6.4	6.4	6.4	19.2	19.2	19.2	19.2
2	KS Statistic 2 ($\times 10^{-5}$)	64.2	63.9	63.9	64.1	65.7	65.0	65.8	65.7
	# Parameters	1	45	31	75	1	45	31	75
	Log-Likelihood	-1464	-1459	-1461	-1456	-1459	-1455	-1455	-1451
	AIC	2930	3008	2985	3062	2920	3000	2971	3051
3	KS Statistic 1 ($\times 10^{-3}$)	7.8	7.0	7.0	6.1	19.5	14.2	12.4	8.9
	KS Statistic 2 ($\times 10^{-5}$)	86.2	86.3	86.0	86.8	88.2	88.1	87.3	88.1
	# Parameters	1	37	53	89	1	37	53	89
	Log-Likelihood	-978	-974	-976	-970	-1016	-1011	-1010	-1006
3	AIC	1959	2021	2057	2117	2034	2095	2126	2189
	KS Statistic 1 ($\times 10^{-3}$)	36.8	34.1	38.1	32.7	18.9	17.8	16.7	17.8
	KS Statistic 2 ($\times 10^{-5}$)	135.5	134.1	134.5	134.5	109.5	108.8	109.8	109.7

where $n = 1, \dots, N$ and T is the total time of the EDA signal in seconds. This results in N Poisson random variables Y_n with means:

$$\mu_n = \frac{T}{N} \left(\lambda_0 + \sum_{k=1}^K \lambda_k e^{-\alpha_k(x_n - \tau_k)} u(x_n - \tau_k) \right) \quad (3)$$

where $x_n = (n - \frac{1}{2}) \frac{T}{N}$ are the mid-time points of each interval. We estimate PP parameters assuming that the sample mean of each Poisson distribution Y_n is equal to the population mean. These parameters can inform us about the interplay dynamics between observed behaviors and underlying EDA (Section 5.3).

4.4. Goodness of Fit Measures

Model evaluation was performed through likelihood and residual analysis. The log-likelihood of observing $\mathbf{n} = [n_1, \dots, n_N]$ SCR arrivals in the subintervals s_n is:

$$\begin{aligned} \mathcal{L} = \mathcal{P}(\mathbf{Y}; \boldsymbol{\theta}) &= \mathcal{P}(Y_1 = n_1, \dots, Y_N = n_N; \boldsymbol{\theta}) \\ &= - \sum_{n=1}^N \lambda(x_n) + \sum_{n=1}^N Y_n \ln \lambda(x_n) - \sum_{n=1}^N Y_n! \end{aligned} \quad (4)$$

Large log-likelihood indicates a better data fit. To compare the different models, we use Akaike's Information Criterion (AIC) [24] $AIC = 2P - 2\log(\mathcal{L})$, where P is the total number of parameters and \mathcal{L} is the likelihood value (Eq. 4). This penalizes the presence of many parameters with smaller values yielding to a better model.

Residual analysis was performed with the Kolmogorov-Smirnov (KS) goodness of fit test that compares two Cumulative Distribution Functions (CDFs) F_1 and F_2 with the statistic $D = \sup_x |F_1(x) - F_2(x)|$. A small value of D indicates that the random samples are likely to be drawn from the same distribution. First, empirical CDF of real SCR occurrence times is compared to the CDF computed from the model with the estimated parameters ("KS Statistic 1"). Second, in order to check whether the major features of the PP can be reproduced, as in [11], we generate data following the estimated PP with the method of thinning [25] and compare empirical CDFs between the real and simulated data ("KS Statistic 2").

These measures can potentially indicate the model and types of external events that better explain the EDA data (Section 5.2).

5. EXPERIMENTS

5.1. Experimental Details

EDA signals were de-noised with a low-pass Blackman filter of 1sec length and SCRs were computed with the LedaLab toolbox [26].

The event times τ_k (Eq. 2) correspond to the observed expert hand-annotated regulatory behaviors. Thus, the child SCR occurrences for each participant were modeled in relation to child self-regulatory, therapist co-regulatory behavior or both resulting in three different models and PP rate functions (Fig. 2d). A similar approach was followed for therapist's SCRs. Our baseline is the homogeneous PP with $\lambda_{baseline}(t) = \lambda_0$ independent of annotated behaviors.

For the LMS estimation of PP parameters, we used a 1sec subinterval (s_n) length. We constrained the parameters in $\lambda_k \in [0.5, 2]$ to avoid negative rate function values and $\alpha_k \in [0, 2]$, since the effect of coded behavior is assumed to diminish within a reasonable time interval. In order to cover the full range of variability and obtain meaningful results, PP simulation was replicated 1,000 times and we report the mean of KS Statistic 2 for all simulations.

In the rest of this section, we provide the goodness of fit results for each participant with the three different PP models. We further compare PP parameters for child and therapist, analyze them with respect to the types of self- and co-regulatory behaviors and use them as features to classify among these types of behaviors. Since there is only instance of each regulatory behavior from Participant 1, we only report goodness of fit results for the sake of completion.

5.2. Goodness of Fit Results

The use of non-homogeneous rate function resulted in increased log-likelihood compared to the homogeneous one (Table 2), since a better data fit occurs, and AIC is larger because of the increased number of parameters. More interestingly, KS statistics tended to be lower for the non-homogeneous PP indicating that SCRs can be better explained by incorporating observed behaviors. The fact that KS Statistic 2 also decreased using the regulatory behaviors suggests that the data can be better reproduced when we take into account these events. Although complex models tend to improve goodness of fit measures, we will discuss next how the model parameters can provide meaningful information about regulatory behaviors (Sections 5.3,5.4), which further implicates the usefulness of the proposed non-homogeneous model compared to the homogeneous one.

5.3. Analysis of Model Parameters

We compared the medians of rate function parameters between child and therapist with the Wilcoxon Rank-Sum test (Table 3). We also produced a 2D plot (Fig. 2) of the exponential amplitude and rate values of Participant 3 marked with the types of self/co-regulatory behaviors (blue 'o' and red 'x' respectively) as defined in Table 1. As expected, the parameter λ_0 of each EDA, stemming from the homogeneous PP part, is similar for self- and co-regulatory behaviors.

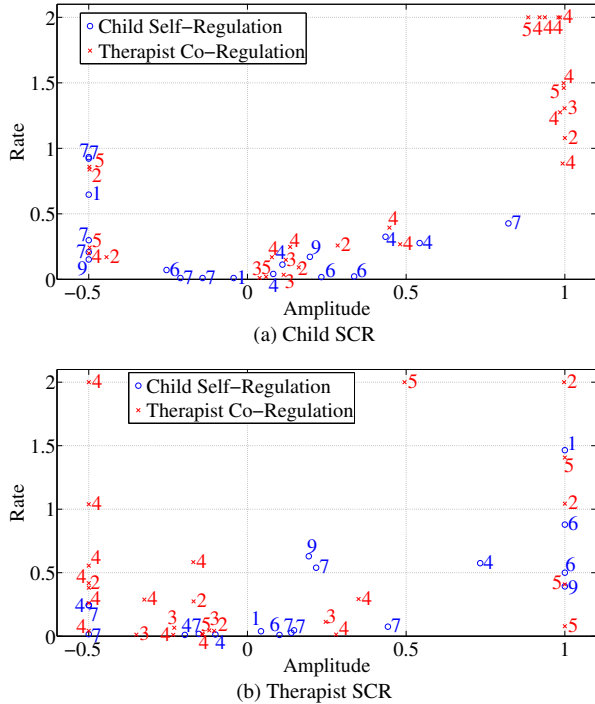


Fig. 2. 2D plot of SCR rate function parameters (exponential amplitude λ_k and rate α_k) with respect to the different types of self/co-regulatory behaviors (as defined in Table 1) for Participant 3.

Child’s exponential amplitude tends to be smaller for self-compared to co-regulation behaviors (Table 3). For Participant 3 (Fig. 2a), high child exponential amplitude mostly occurs when the therapist followed upon the child’s distress or physically comforted the child (co-regulation 4 and 5). Child’s comfort seeking (co-regulation 7,9) resulted in lower exponential amplitudes than tension release (co-regulation 4). This could be due to either the motion involved in tension release, or to higher actual physiological arousal. Low SCR rate after assistance seeking events (self-regulation 9) could stem from the child’s loss of interest or reduced effort.

Self-regulation resulted in higher median of the therapist’s exponential amplitude than co-regulatory behavior. Interestingly, for Participant 3 (Fig. 2b), some of the child’s orientation to therapist and assistance seeking behaviors (self-regulation 7,9) provide higher amplitude values than the child’s tension release (self-regulation 4).

Finally, exponential change rate tended to be higher when child’s SCR are modeled with therapist’s regulatory behaviors and vice-versa, implying longer effect of the external stimuli to the EDA.

5.4. Classification of Self/Co-Regulation Events

We classified the different types of child self-regulatory behaviors (Table 1) based on the estimated rate function parameters of child EDA, therapist EDA and both. Our feature vector for a sample event k was the 2-dimensional vector $[\lambda_k \ \alpha_k]$ of the child or therapist SCR parameters, or 4-dimensional vector including both. Same experiments were performed for the therapist co-regulatory behaviors.

Our setup involved a within-participant leave-one-instance-out cross-validation, where “instance” is a self/co-regulatory behavior. Due to small data dimensionality, no feature selection was used and classification was performed with a K-NN classifier with 1 or 3 nearest neighbors. If we had more than 2 samples per class, we optimized the number of neighbors with a held-out set, i.e. one instance for test,

Table 3. Estimated values of non-homogeneous Poisson Process model parameters of child and therapist Skin Conductance Responses (SCRs) based on self/co-regulatory behaviors (λ_0 : baseline amplitude, λ : median amplitude, α : median rate). P-values are computed with a one-sided Wilcoxon Rank-Sum test on the medians.

Participant	Metric	Child SCR			Therapist SCR		
		Child Self-Reg.	Therapist Co-Reg.	P-value	Child Self-Reg.	Therapist Co-Reg.	P-value
2	λ_0	0.761	0.760	—	0.746	0.734	—
	λ	0.014	0.075	0.197	0.399	0.306	0.500
	α	0.340	0.809	0.089	0.457	0.745	0.469
3	λ_0	0.729	0.704	—	0.915	0.931	—
	λ	-0.092	0.366	0.003	0.143	-0.156	0.078
	α	0.162	0.616	0.006	0.158	0.281	0.179

Table 4. Unweighted classification accuracy (%) of the different types of child self and therapist co-regulatory behaviors.

Participant	Classification Labels	Chance	Child SCR	Therapist SCR	Child/Therapist SCR
			SCR	SCR	SCR
2	Child Self-Reg.	33.33	27.45	60.78	64.71
	Therapist Co-Reg.	33.33	81.90	37.14	48.57
3	Child Self-Reg.	20.00	44.76	8.57	21.43
	Therapist Co-Reg.	25.00	19.58	24.58	36.67

one for dev and the rest for train, otherwise we used 1-NN. We also omitted classes with only one sample from the experiments.

Classification results (Table 4) suggest that externally observed behaviors embedded in our model provide useful information with respect to bio-behavioral interpersonal regulatory mechanisms. It is also noteworthy that in some cases, e.g. Participant 2, information from inner physiological cues of the child can predict the observed annotated behavior of the therapist and vice versa.

6. DISCUSSION

Developing measures that quantify the effect of therapy to a child’s regulatory behavior and physiology can afford insights into the mechanisms of therapeutic change. One could hypothesize that an intervention’s beneficial impact is expressed through a therapist enabling a child to better regulate his or her physiological and behavioral responses. This could be manifested by moderate SCR rate changes and fast recovery to baseline, resulting in small exponential amplitude and large exponential change rate in our model.

Furthermore, given that different therapists might elicit different behaviors from a child, a good child-therapist match is important in a therapeutic context. Child-therapist co-regulation could occur when one’s behavioral events explain better the other’s physiological state, quantified with the goodness of fit measures we studied.

7. CONCLUSIONS AND FUTURE WORK

We propose a non-homogeneous PP model of SCR occurrences whose rate function is influenced by observable behavior. This has relevance to ASD interventions, during which child and therapist EDA is modeled in relation to expert hand-annotated regulatory behaviors. We evaluated our approach with goodness of fit tests and analysis of resulting model parameters. Classification was performed across different types of regulatory behavior based on estimated parameters. Our results indicate that child and therapist physiological state is interdependent, associated with observable behavior and can differ across various self/co-regulatory behavior types.

In the future, we plan to include more child-therapist participants and observe bio-behavioral patterns at different therapy stages. We will also incorporate SCR amplitude and recovery time information and jointly model child and therapist EDA. Finally, more point processes and parameter estimation techniques will be explored.

Acknowledgment: Thanks to NSF and NIH for funding.

8. REFERENCES

- [1] S. J. Rogers and L. A. Vismara, "Evidence-based comprehensive treatments for early autism," *Journal of Clinical Child & Adolescent Psychology*, vol. 37, no. 1, pp. 8–38, 2008.
- [2] B. Reichow and F. R. Volkmar, "Social skills interventions for individuals with autism: evaluation for evidence-based practices within a best evidence synthesis framework," *Journal of Autism and Developmental Disorders*, vol. 40, no. 2, pp. 149–166, 2010.
- [3] R. Thompson, "Emotion regulation: A theme in search of definition," *Monographs of the Society for Research in Child Development*, vol. 59, no. 2-3, pp. 25–52, 1994.
- [4] A. C. Gulsrud, L. B. Jahromi, and C. Kasari, "The coregulation of emotions between mothers and their children with autism," *Journal of Autism and Developmental Disorders*, vol. 40, no. 2, pp. 227–237, 2010.
- [5] N.J. Minshew and D.L. Williams, "The new neurobiology of autism: cortex, connectivity, and neuronal organization," *Archives of Neurology*, vol. 64, no. 7, pp. 945–950, 2007.
- [6] C. Kasari and L. Lawton, "New directions in behavioral treatment of autism spectrum disorders," *Current Opinion in Neurology*, vol. 23, no. 2, pp. 137–143, 2010.
- [7] M. S. Goodwin, J. Groden, W. F. Velicer, L. P. Lipsitt, M. G. Baron, S. G. Hofmann, and G. Groden, "Cardiovascular arousal in individuals with autism," *Focus on autism and other developmental disabilities*, vol. 321, pp. 100–123, 2006.
- [8] H. D. Critchley, "Electrodermal responses: what happens in the brain," *Neuroscientist*, vol. 8, pp. 132–142, 2002.
- [9] R. W. Picard, "Future affective technology for autism and emotion communication," *Phil. Trans. R. Soc.*, vol. 364, pp. 3575–3584, 2009.
- [10] S. Narayanan and P. G. Georgiou, "Behavioral Signal Processing: Deriving Human Behavioral Informatics from Speech and Language," *Invited paper. Proceedings of the IEEE*, vol. 101, no. 5, pp. 1203–1233, 2013.
- [11] Y. Ogata, "Statistical models for earthquake occurrences and residual analysis for point processes," *Journal of the American Statistical Association*, vol. 83, no. 401, pp. 9–27, 1988.
- [12] W. A. Massey, G. A. Parker, and W. Whitt, "Estimating the parameters of a nonhomogeneous poisson process with linear rate," *Telecommunication Systems*, vol. 5, no. 2, pp. 361–388, 1996.
- [13] S. A. Hossain and R.C. Dahiya, "Estimating the parameters of a non-homogeneous poisson-process model for software reliability," *IEEE Transactions on Reliability*, vol. 42, no. 4, pp. 604 – 612, 1993.
- [14] R. Barbieri, E. C. Matten, A. A. Alabi, and E. N. Brown, "A point-process model of human heartbeat intervals: new definitions of heart rate and heart rate variability," *American Journal of Physiology - Heart and Circulatory Physiology*, vol. 288, no. 1, pp. 424–435, 2005.
- [15] C. C. Lee, A. Katsamanis, M. P. Black, B. R. Baucom, A. Christensen, P. G. Georgiou, and S. S. Narayanan, "Computing vocal entrainment: A signal-derived PCA-based quantification scheme with application to affect analysis in married couple interactions," *In Press: Computer Speech and Language*, 2012.
- [16] D. Bone, M. P. Black, C. C. Lee, M. E. Williams, P. Levitt, S. Lee, and S. Narayanan, "Spontaneous-speech acoustic-prosodic features of children with autism and the interacting psychologist," *Proceedings of InterSpeech, Portland, OR*, 2012.
- [17] D. Bone, C. C. Lee, T. Chaspari, M. Black, M. Williams, S. Lee, P. Levitt, and S. Narayanan, "Acoustic-prosodic, turn-taking, and language cues in child-psychologist interactions for varying social demand," *Proceedings of InterSpeech, Lyon, France*, 2013.
- [18] R. Gupta, C. C. Lee, D. Bone, S. Lee, and S. Narayanan, "Acoustical analysis of engagement behavior in children," *Proceedings of Workshop on Child, Computer and Interaction (WOCCI)*, 2012.
- [19] Z. Yang, A. Metallinou, and S. Narayanan, "Toward body language generation in dyadic interaction settings from interlocutor multimodal cues," *Proceedings of ICASSP, Vancouver, Canada*, 2013.
- [20] M. Z. Poh, N. C. Swenson, and R. W. Picard, "A wearable sensor for unobtrusive, long-term assessment of electrodermal activity," *IEEE Trans. on Biomedical Engineering*, vol. 57, pp. 1243–1252, 2010.
- [21] S. A. Schoen, L. J. Miller, B. Brett-Green, and S. L. Hepburn, "Psychophysiology of children with autism spectrum disorder," *Research in Autism Spectrum Disorders*, vol. 2, no. 3, pp. 417–429, 2008.
- [22] B. E. Hubert, B. Wicker, E. Monfardini, and C. Deruelle, "Electrodermal reactivity to emotion processing in adults with autistic spectrum disorders," *Autism*, vol. 13, no. 1, pp. 9–19, 2009.
- [23] M.E. Dawson, A. M. Schell, and D. L. Filion, "The Electrodermal System," in *Handbook of psychophysiology*, J. T. Cacioppo, L. G. Tassinary, and G. G. Berntson, Eds., pp. 159–181. New York: Cambridge University Press, 3rd edition, 2007.
- [24] H. Akaike, "Information theory and an extension of the maximum likelihood principle," in *Selected Papers of Hirotugu Akaike*, P. Parzen, Tanabe K., and Kitagawa G., Eds., pp. 199–213. Springer New York, 1998.
- [25] P. A. Lewis and G. B. Shedler, "Simulation of nonhomogeneous poisson processes by thinning," *Naval Research Logistics Quarterly*, vol. 26, no. 3, pp. 403–413, 1979.
- [26] M. Benedek and C. Kaernbach, "Decomposition of skin conductance data by means of nonnegative deconvolution," *Psychophysiology*, vol. 47, no. 4, pp. 647658, 2010.